

# Relativistic Two-component Double Ionization Potential Equation-of-Motion Coupled Cluster with the Dirac–Coulomb–Breit Hamiltonian

Run R. Li,<sup>1</sup> Stephen H. Yuwono,<sup>1</sup> Marcus D. Liebenthal,<sup>1</sup> Tianyuan Zhang,<sup>2</sup> Xiaosong Li,<sup>2</sup> and A. Eugene DePrince III<sup>1, a)</sup>

<sup>1)</sup>*Department of Chemistry and Biochemistry, Florida State University, Tallahassee, FL 32306-4390, USA*

<sup>2)</sup>*Department of Chemistry, University of Washington, Seattle, WA 98195, USA*

We present an implementation of relativistic double-ionization-potential (DIP) equation-of-motion coupled-cluster (EOMCC) with up to 4-hole–2-particle ( $4h2p$ ) excitations that makes use of the molecular mean-field exact two-component (mmfX2C) framework. We apply mmfX2C-DIP-EOMCC to several neutral atoms and diatomic molecules to obtain the ground and first few excited states of the corresponding di-cation species, and we observe excellent agreement (to within 0.001 eV) between double ionization potentials (IPs) obtained from mmfX2C- and four-component DIP-EOMCC calculations that include 3-hole–1-particle ( $3h1p$ ) excitations, with either the Dirac–Coulomb or Dirac–Coulomb–Gaunt Hamiltonians. We also compare double IPs for mmfX2C-DIP-EOMCC calculations with the full Dirac–Coulomb–Breit (DCB) Hamiltonian to those from experiment. The mmfX2C-DIP-EOMCC with  $3h1p$  excitations leads to errors in absolute double IPs that are larger than 0.1 eV, whereas the addition of  $4h2p$  excitations reduces these errors dramatically, often by an order of magnitude or more.

## I. INTRODUCTION

High-accuracy simulations of ground-state electronic structure often rely on the coupled-cluster (CC) family of methods.<sup>1–7</sup> The popularity of CC approaches stems from their systematic improvability and rapid convergence to the full configuration interaction (CI) limit [from CC with single and double excitations (CCSD)<sup>8,9</sup> to CCSD plus triple excitations (CCSDT)<sup>10,11</sup> and beyond], as well as the size-extensivity and separability of the CC energy, regardless of the level at which the cluster operator is truncated. For the description of electronically excited states, CC theory can be extended using various approaches that inherit the desirable properties of CC, including equation-of-motion (EOM)<sup>12–14</sup> or linear response (LR) CC,<sup>15–21</sup> as well as the related symmetry-adapted cluster (SAC) CI framework.<sup>22</sup> The strengths of these approaches aside, certain situations remain challenging, such as the description of systems that exhibit multi-reference (MR) character, examples of which include open-shell radicals and diradicals, potential energy curves along bond-breaking coordinates, transition metal complexes with multiple unpaired electrons, and excited states that are dominated by two-electron transitions.

Multi-reference CC approaches seem to be the natural choice to treat systems with MR character, but they come with various complications such as intruder states, size extensivity issues, and the ambiguity in the specification of the MRCC wave function *ansatz* itself (see, *e.g.*, Refs. 6,7,23–25 for reviews of MRCC approaches). On the other hand, a number of strategies from the single-reference (SR) CC realm can be used to build wave functions for systems with MR character. These approaches could be as direct as the application of CC/EOMCC on top of a broken-symmetry Hartree–Fock (HF)

reference function or the use of spin-flip CC/EOMCC,<sup>26–29</sup> which exploits the mostly SR nature of a high-spin HF configuration. While straightforward, such strategies may be problematic as the resulting wave functions can exhibit significant spin contamination. An alternative approach is given by the use of particle-non-conserving operators that add or remove electrons from a closed-shell  $N$ -electron state that is well-described by SR CC; examples in this domain include the ionization potential (IP)<sup>30–39</sup> or electron attachment (EA)<sup>37–42</sup> EOMCC, which take inspiration from Fock-space CC methods. If the  $N$ -electron state is described using SR CC built on top of a restricted HF (RHF) configuration, the open-shell wave function remains spin-adapted, and the expected degeneracy structure will be conserved. In this work, we explore the double IP (DIP)<sup>43–50</sup> EOMCC method, which allows, for example, the description of  $p^4$  or  $d^8$  electron configurations generated from the corresponding  $p^6$  or  $d^{10}$  closed-shell references, respectively, as well as direct determination of double ionization energies.

In addition to the accurate treatment of electronic correlation effects, quantitative predictions involving open-shell species may also require a sophisticated treatment of spin-free and spin-dependent relativistic effects, particularly when studying spin-orbit coupling dependent phenomena. For these purposes, the four-component (4c) Dirac–Coulomb–Breit (DCB) Hamiltonian offers the most complete description of relativistic effects in fermionic systems. However, the DCB Hamiltonian contains both the electronic and positronic degrees of freedom, the latter of which are not directly relevant to quantum chemistry applications and lead to unnecessary increases in the cost and complexity of simulations on large molecular systems. As such, approximations that effectively decouple the electronic and positronic degrees of freedom are desirable. One such method that has gained popularity in the past couple of decades is the exact two-component (X2C) approach,<sup>51–74</sup> which downfolds the relativistic physics in the 4c space into a smaller two-component (2c) space with-

<sup>a)</sup>Electronic mail: adeprince@fsu.edu

out much loss in accuracy.

Several applications of DIP-EOMCC can be found in the literature that incorporate relativistic effects through the X2C framework or other means. For example, Wang and coworkers<sup>75,76</sup> used effective core potential (ECP) to include the scalar relativistic effect at the mean-field level and applied a one-electron relativistic Hamiltonian in the post-HF treatment. More recently, Piecuch and coworkers<sup>50</sup> have implemented DIP-EOMCCSDT with up to 4-hole–2-particle ( $4h2p$ ) excitations included in the EOMCC operator on top of the CCSDT ground-state reference, as well as an approximate form of this method, in combination with a spin-free relativistic Hamiltonian. Probably the most sophisticated treatment of relativistic effects in this context has been provided by Pathak and coworkers,<sup>77,78</sup> who developed 4c DIP-EOM-CCSD with the Dirac–Coulomb (DC) and Dirac–Coulomb–Gaunt (DCG) Hamiltonians at both the HF and post-HF levels; these methods were subsequently used to calculate the DIPs of alkaline metal atoms, rare gas atoms, and a few diatomic molecules. In the present work, we push the correlation and relativistic treatments in DIP-EOMCC to include both high-order correlation effects (*i.e.*, DIP-EOMCCSDT with  $4h2p$  transitions) and the full DCB Hamiltonian within the molecular mean-field X2C (mmfX2C) approach.

The remainder of this paper is organized as follows: Section II provides the relevant details of the X2C relativistic framework and CC/DIP-EOMCC correlation treatment. The details of our computations are presented in Sec. III, after which the results of these computations are discussed in Section IV. Lastly, Sec. V provides some concluding remarks.

## II. THEORY

### A. The X2C framework

The relativistic many-electron Hamiltonian takes the form

$$\hat{H} = \sum_i \left[ (\beta - \mathbb{1}_4)mc^2 + c(\alpha_i \cdot \hat{\mathbf{p}}_i) + \sum_A \hat{V}_{iA} \right] + \sum_{i < j} \left[ \frac{1}{r_{ij}} - \frac{\alpha_i \cdot \alpha_j}{r_{ij}} + \frac{1}{2} \left( \frac{\alpha_i \cdot \alpha_j}{r_{ij}} - \frac{\alpha_i \cdot \mathbf{r}_{ij} \alpha_j \cdot \mathbf{r}_{ij}}{r_{ij}^3} \right) \right] \quad (1)$$

where  $m$  is mass of the electron,  $c$  is the speed of light,  $\mathbb{1}_4$  is the 4c identity matrix,  $\hat{\mathbf{p}}_i$  is the momentum operator for electron  $i$ ,  $\alpha_i$  and  $\beta$  are the Dirac matrices,  $\hat{V}_{iA}$  is the potential energy operator for electron  $i$  in the field of nucleus  $A$ , and  $r_{ij}$  represents the distance between electrons  $i$  and  $j$ . The three two-electron terms in Eq. 1 are referred to as the Coulomb, Gaunt, and gauge terms. When accounting for all three, we refer to  $\hat{H}$  as the full Dirac–Coulomb–Breit (DCB) Hamiltonian. Approximations to the DCB Hamiltonian include the Dirac–Coulomb (DC) Hamiltonian, which accounts for only the Coulomb term ( $r_{ij}^{-1}\mathbb{1}_4$ ), and the Dirac–Coulomb–Gaunt (DCG) Hamiltonian, which accounts for the Coulomb term and the Gaunt term  $[-\alpha_i \cdot \alpha_j (r_{ij})^{-1}]$ .

In the mmfX2C approach, one begins with a 4c-HF calculation carried out with the DC, DCG, or DCB relativistic Hamiltonian. The electronic molecular spinors obtained via this procedure define the unitary 4c to 2c transformation, which is applied to the Fock operator and the Coulomb part of the two-electron operator. The subsequent correlation treatment is then carried out with these operators in the transformed 2c basis. This procedure ensures that two-electron relativistic effects are captured self-consistently at the mean-field level, while it is assumed that correlation effects stemming from the Gaunt or gauge terms will be small and can be neglected in the post-HF part of the calculation. In this work, the notations DC-/DCG-/DCB-X2C refer to mmfX2C-based calculations employing the appropriate relativistic Hamiltonians.

In addition to the mmfX2C approach, we also consider the simpler one-electron X2C (1eX2C) in which a unitary 4c to 2c transformation is applied directly to the one-body part in Eq. 1 (the core Hamiltonian). The HF and correlation treatments are carried out in the resulting 2c basis, with a non-relativistic Coulomb operator. The missing two-body spin-orbit interaction effects can be approximated by scaling the spin-orbit part of the core Hamiltonian using a screened nuclear spin-orbit (SNSO) factor.<sup>79</sup> In this work, the 1eX2C procedure uses the row-dependent factors parametrized for the DCB Hamiltonian in Ref. 80. For additional detailed comparisons of the mmfX2C and 1eX2C approaches, we refer the reader to Refs. 72, 81, 82, and the references contained therein.

### B. DIP-EOMCC Theory

In this section, we provide the pertinent details of the CC and DIP-EOMCC approaches, the latter of which is used to model doubly ionized states. Throughout the discussion, the labels  $i_1, i_2, \dots$  and  $a_1, a_2, \dots$  refer to molecular spinors that are occupied and unoccupied in the reference (1eX2C- or mmfX2C-HF) configuration. We also make use of the Einstein summation convention, where repeated lower and upper indices imply summation.

In the CC approach, the ground-state electronic wave function for an  $N$ -electron system is expanded as

$$|\Psi_0^{(N)}\rangle = \exp(\hat{T})|\Phi_0\rangle \quad (2)$$

where  $|\Phi_0\rangle$  is the reference configuration. The cluster operator,  $\hat{T}$ , is expanded in terms of products of particle-conserving excitation operators, *i.e.*,

$$\hat{T} = \sum_{n=1}^M \hat{T}_n, \quad \hat{T}_n = \left( \frac{1}{n!} \right)^2 t_{a_1 \dots a_n}^{i_1 \dots i_n} \prod_{k=1}^n (\hat{a}^{a_k} \hat{a}_{i_k}) \quad (3)$$

where  $t_{a_1 \dots a_n}^{i_1 \dots i_n}$  are the cluster amplitudes, and the symbols  $\hat{a}^{a_k}$  and  $\hat{a}_{i_k}$  represent creation and annihilation operators for molecular spinors  $a_k$  and  $i_k$ , respectively. Here, the parameter  $M$  determines the level in the CC hierarchy of methods, and the full CC ( $\equiv$  full CI) limit is reached when  $M = N$  (where  $N$  is the number of electrons). In this work, we are concerned

with the  $M = 2$  (CCSD) and  $M = 3$  (CCSDT) levels. The cluster amplitudes are determined in the usual projective way, *i.e.*, by solving

$$\langle \Phi_{i_1 \dots i_n}^{a_1 \dots a_n} | \bar{H} | \Phi_0 \rangle = 0 \forall | \Phi_{i_1 \dots i_n}^{a_1 \dots a_n} \rangle, n = 1, 2, \dots, M. \quad (4)$$

where we have introduced the similarity-transformed Hamiltonian,  $\bar{H} = e^{-\hat{T}} H e^{\hat{T}}$ . In Eq. 4, the symbol  $| \Phi_{i_1 \dots i_n}^{a_1 \dots a_n} \rangle$  refers to a determinant of spinors that is  $n$ -tuply substituted relative to the reference determinant. Once the amplitudes have been determined, the CC energy is given by the expectation value of  $\bar{H}$  with respect to the reference configuration,

$$E_0 = \langle \Phi_0 | \bar{H} | \Phi_0 \rangle. \quad (5)$$

Given optimal cluster amplitudes obtained from solving Eq. 4, excited-state information can be determined using the EOMCC approach, wherein the excited-state energies are given by the eigenvalues of the similarity-transformed Hamiltonian. One of the major strengths of the EOMCC formalism is that one has great flexibility in terms of the many-particle basis in which  $\bar{H}$  is expanded, and different choices give access to different particle-number of spin-symmetry sectors of Fock space (see Ref. 29 for a review on this topic). For example, energies and wave functions of the  $(N - 2)$ -electron (*i.e.*, doubly ionized) states can be obtained from DIP-EOMCC, where the  $K$ -th doubly ionized state ( $K > 0$ ) is parametrized as

$$| \Psi_K^{(N-2)} \rangle = \hat{R}_K | \Psi_0^{(N)} \rangle = \hat{R}_K \exp(\hat{T}) | \Phi_0 \rangle, \quad (6)$$

In the DIP-EOMCC approach, the excitation operator  $\hat{R}_K$  is taken to be a linear, non-particle-conserving operator that removes two electron from the  $N$ -electron state. We have

$$\hat{R}_K = \sum_{n=2}^{M+1} \hat{R}_{K,n}, \hat{R}_{K,n} = \frac{1}{n!(n-2)!} r_{K,a_3 \dots a_n}^{i_1 \dots i_n} \hat{a}_{i_2} \hat{a}_{i_1} \prod_{k=3}^n (\hat{a}^{a_k} \hat{a}_{i_k}), \quad (7)$$

where  $M$  is a truncation level that, in this work, is consistent with that chosen in Eq. 4. For  $M = 2$  and  $M = 3$ , Eq. 7 leads to the DIP-EOMCCSD and DIP-EOMCCSDT approaches, which include up to three-hole-one-particle ( $3h1p$ ) or four-hole-two-particle ( $4h2p$ ) transitions in  $\hat{R}_K$ , respectively. Inserting Eq. 6 into the Schrödinger equation gives

$$\bar{H} \hat{R}_K | \Phi_0 \rangle = E_K \hat{R}_K | \Phi_0 \rangle \quad (8)$$

which is a non-Hermitian eigenvalue problem that can be solved for the energies of the doubly ionized states,  $E_K$ . The double IP values are then given by  $\omega_K = E_K - E_0$ .

### III. COMPUTATIONAL DETAILS

Section IV begins with a direct comparison between the DIP values determined using mmfX2C-DIP-EOMCCSD and 4c DIP-EOMCCSD using various relativistic Hamiltonians. The 4c DIP-EOMCCSD data for this evaluation were taken from Ref. 78. For consistency, the present mmfX2C-based

calculations use the same basis sets and truncation scheme as were used in Ref. 78. All basis sets are of at least triple-zeta quality, mostly in the Dyall family, with high-lying virtual spinors (with orbital energies greater than  $500 E_h$ ) excluded from the correlated part of the calculation. All electrons were correlated in these calculations. The reader is referred to Table I of Ref. 78 for additional details. Subsequent studies using mmfX2C- and 1eX2C-DIP-EOMCC examined a variety of basis sets, including the X2C-SVPall-2c and X2C-TZVPPall-2c,<sup>83</sup> Dyall.acv<sup>nz</sup>,<sup>84-89</sup> and ANO-RCC-VnZP<sup>90,91</sup> families, where  $n$  is the cardinal number. Unlike above, these studies were carried out using the full set of virtual spinors. We also use the frozen-core approximation, where only electrons in the valence shell plus one inner shell are correlated.

The X2C-DIP-EOMCCSD calculations were carried out using the Cholesky decomposition (CD) approximation to the non-relativistic electron repulsion integrals (ERIs), with a decomposition threshold of  $1 \times 10^{-4} E_h$ . It is well known that use of the CD approximation in ground-state CCSD calculations is an effective way to reduce memory requirements, for example, by constructing and storing only subblocks of the four-virtual-index part of the ERI tensor.<sup>92</sup> On the other hand, the EOM part of DIP-EOMCCSD does not depend on any parts of the ERI tensor involving more than three virtual spinor labels, so there is less direct benefit to the use of the CD approximation in EOM part of the DIP-EOMCCSD algorithm. The only  $ov^3$ -sized ERI term (where  $o$  and  $v$  represent the number of occupied and virtual spinors, respectively) is used in the construction of smaller  $\bar{H}$  intermediate quantities that enter into the iterative parts of the EOM algorithm, which itself only involves quantities with two or fewer virtual spinor labels. Calculations carried out at the X2C-DIP-EOMCCSDT level of theory did not make use of the CD approximation to the ERI tensor.

All calculations reported in this work were performed with the DIP-EOMCC code implemented in a development branch of Chronus Quantum<sup>93</sup> using the TiledArray tensor algebra framework<sup>94</sup>. Equations and corresponding TiledArray expressions were generated using the  $p^\dagger q$  package,<sup>95,96</sup> and expressions for DIP-EOMCCSD  $\bar{H}$  intermediates were modified to account for the use of the CD approximation.

### IV. RESULTS AND DISCUSSION

We begin with an assessment of the agreement between double IPs obtained from the present mmfX2C-DIP-EOMCCSD calculations and literature values computed using four-component (4c) DIP-EOM-CCSD.<sup>78</sup> Table I contains vertical double IP values for noble gas atoms and diatomic molecules that were computed using these methods, with three different relativistic Hamiltonians. As mentioned above and discussed in Ref. 78, hydrogen atoms are described using the aug-cc-pVTZ basis set, while all other atoms are described using various Dyall-type basis sets of triple-zeta quality. In all cases, all electrons were correlated, but virtual molecular spinors with energies above  $500 E_h$  were excluded from the correlated parts of the calculations. Using the Dirac-

Coulomb Hamiltonian, we find excellent agreement between double IPs obtained from DC-X2C- and 4c-DIP-EOM-CCSD, with the largest discrepancies being only 0.003 eV in magnitude. As such, we are able to conclude the following. First, the error introduced via the CD approximation in mmfX2C-DIP-EOMCC is negligible. Second, because two-electron relativistic effects are only captured at the mean-field level in mmfX2C-DIP-EOMCC, correlation effects stemming from the relativistic two-electron part of the Hamiltonian must be small for these systems. Reference 78 also considered 4c-DIP-EOMCCSD calculations on the krypton atom that included the Gaunt term in the Hamiltonian; we find excellent agreement between 4c- and DCG-X2C-DIP-EOMCCSD double IPs in this case. The changes in the double IPs induced by the Gaunt term are consistent between these methods to within 0.001 eV or less. For krypton and the remaining systems, DCG-X2C-DIP-EOMCCSD calculations indicate that the Gaunt term always lowers the double IPs, by as little as -0.004 eV (for the  $^1\Sigma^-$  state of  $\text{Cl}_2$ ) or as much as -0.043 eV (for the  $^1S_0$  state of xenon atom), with the average change being -0.017 eV. On the other hand, the gauge term in DCB-X2C-DIP-EOMCCSD universally raises the double IPs, by a fairly consistent amount for each species (0.001 - 0.005 eV). For a given atom or molecule, the largest deviations between the gaunt contributions to the double IPs for different states are no more than 0.001 eV.

Given the excellent agreement between mmfX2C- and 4c-DIP-EOMCCSD, it is also interesting to consider the degree to which different X2C schemes (*i.e.*, 1eX2C versus mmfX2C) provide consistent double IP values. Table II provides the mean absolute deviation (MAD) between 1eX2C- and DCB-X2C-DIP-EOMCCSD derived double IPs for the same systems and states considered in Table I. Here, we use the row-dependent DCB-parameterized SNSO<sup>80</sup> scheme in the 1eX2C procedure. Unlike in Table I, calculations are carried out using ANO-RCC-*n*ZVP (*n* = D, T, Q) basis sets, all virtual orbitals are correlated in the calculations, and we only correlate the electrons in the valence shell plus one inner shell. From these data, it appears that double IP values obtained using different X2C schemes can differ by as much as 0.1 eV. These deviations decrease substantially (by more than a factor of three) when increasing the basis set from double-zeta to triple-zeta quality, but the deviations grow slightly when increasing the basis set from triple-zeta to quadruple-zeta quality. This behavior is similar to the behavior observed in Ref. 82 for single IP values computed using 1eX2C- and DCB-X2C-IP-EOMCCSD. In that case, we observe that, for contracted basis sets such as the ANO-RCC family, 1eX2C- and DCB-X2C-IP-EOMCCSD derived IP values sometimes differed by as much as a few hundredths of 1 eV, but the agreement between these relativistic treatments generally improved with increased basis set size. In Ref. 82, the discrepancy was traced to the recontraction of the basis after the X2C-HF procedure. Clearly, a similar discrepancy exists in the case of the double IPs considered here, although, the current problem seems a bit worse. Not only are the observed energy differences significantly larger than those observed in Ref. 82, they are also much larger than the difference in dou-

TABLE I. Double ionization potentials (eV) from X2C- and 4c-DIP-EOMCCSD calculations carried out using different relativistic Hamiltonians. Basis set and virtual space truncation information can be found in Ref. 78.

State	Dirac–Coulomb		+Gaunt		+gauge X2C	
	X2C	4c	X2C	4c		
Ar	$^3P_2$	43.448	43.448	-0.008	-	0.002
	$^3P_1$	43.595	43.596	-0.014	-	0.002
	$^3P_0$	43.656	43.657	-0.016	-	0.002
	$^1D_2$	45.241	45.241	-0.012	-	0.002
	$^1S_0$	47.695	47.694	-0.012	-	0.002
Kr	$^3P_2$	38.342	38.341	-0.012	-0.012	0.004
	$^3P_1$	38.930	38.930	-0.024	-0.024	0.004
	$^3P_0$	39.027	39.028	-0.023	-0.023	0.004
	$^1D_2$	40.218	40.218	-0.023	-0.022	0.004
	$^1S_0$	42.566	42.566	-0.027	-0.027	0.004
Xe	$^3P_2$	33.016	33.016	-0.014	-	0.004
	$^3P_1$	34.267	34.268	-0.031	-	0.004
	$^3P_0$	34.064	34.065	-0.021	-	0.005
	$^1D_2$	35.221	35.222	-0.031	-	0.005
	$^1S_0$	37.656	37.659	-0.043	-	0.005
Cl <sub>2</sub>	$^3\Sigma^-$	31.394	31.397	-0.007	-	0.002
	$^1\Delta$	31.905	31.907	-0.008	-	0.002
	$^1\Sigma^+$	32.292	32.294	-0.008	-	0.002
	$^1\Sigma^-$	33.322	33.319	-0.004	-	0.001
Br <sub>2</sub>	$^3\Sigma_{g0}^-$	28.473	28.473	-0.011	-	0.003
	$^3\Sigma_{g1}^-$	28.635	-	-0.015	-	0.003
	$^1\Delta_{g2}$	29.041	29.041	-0.015	-	0.003
	$^1\Sigma_{g0}^+$	29.519	29.519	-0.019	-	0.003
HBr	$^3\Sigma^-$	32.756	32.757	-0.011	-	0.003
	$^1\Delta$	34.143	34.143	-0.013	-	0.003
	$^1\Sigma^+$	35.429	35.429	-0.015	-	0.003
HI	$^3\Sigma_0^-$	29.173	29.174	-0.013	-	0.004
	$^1\Sigma_1^-$	29.411	29.412	-0.018	-	0.003
	$^1\Delta$	30.480	30.481	-0.018	-	0.004
	$^1\Sigma^+$	31.800	31.801	-0.022	-	0.004

TABLE II. Mean absolute deviations (eV) between 1eX2C- and DCB-X2C-DIP-EOMCCSD derived double IP values and gaps between the lowest double IP value and the higher values.

Assessed quantity	DZVP	TZVP	QZVP
Double IPs	0.104	0.031	0.034
Energy gaps	0.024	0.031	0.015

ble IPs from X2C- and 4c-DIP-EOMCCSD provided in Table I. Table II also provides mean absolute deviations in energy gaps (the difference between the lowest-energy double IP for a given atom or molecule and the higher-energy double IPs). 1eX2C- and DCB-X2C-DIP-EOMCCSD again provide results that differ on the order of 0.01 eV or more, suggesting that this basis set recontraction issue does not benefit much from a cancellation of errors when looking at energy differences. Therefore, we focus on the more complete mmfX2C framework for the remainder of this work.

We now assess the accuracy of double IPs from DCB-X2C-DIP-EOMCC calculations, as compared to experimentally de-

terminated values. Figure 1 provides errors in predicted double IP values obtained from DCB-X2C-DIP-EOMCCSD calculations carried out in various contracted (ANO-RCC-<sup>90,91</sup> and x2c-type<sup>83</sup>) and uncontracted (Dyall-type<sup>84-89</sup>) basis sets. Results are provided for the same species and states tabulated in Table I, with experimental data taken from Refs. 97–101. The raw computed and experimentally obtained double IP values can be found in the Supporting Information. Before analyzing the results of our DIP calculations, it is worth noting that previously reported DIP values<sup>50,78</sup> for the Cl<sub>2</sub>, Br<sub>2</sub>, HBr, and HI diatomics correspond to purely electronic vertical transitions, whereas the experimental double IPs reported in Refs. 98–101 are extracted from vibrationally resolved threshold photoelectron spectra, which capture adiabatic transitions that account for the zero-point vibrational energy (ZPVE) differences between the neutral and dication states. The estimates for ZPVE effects, calculated as the differences between the harmonic vibrational frequencies of Cl<sub>2</sub>, Br<sub>2</sub>, HBr, and HI in their lowest dication and neutral states,<sup>97–101</sup> amount to –0.002 (Br<sub>2</sub>), –0.027 (Cl<sub>2</sub>), –0.047 (HI), and –0.123 (HBr) eV. Accurate comparison against experimental data should take into account the geometrical relaxation and ZPVE effects, but in this work we report the purely electronic vertical DIP values consistent with past theoretical treatments.

As was the case for the data presented in Table II, the data in Fig. 1 were generated by calculations that made use of the frozen core approximation (*i.e.*, we only correlate electrons in the valence shell plus one inner shell), with all virtual orbitals correlated. We begin by considering the convergence of the double IP values toward the complete basis set limit, with the truncated ANO-RCC- $n$ ZVP ( $n = D, T, Q$ ) and full ANO-RCC basis sets. We find that the double IPs are severely underestimated within the double-zeta basis, with a mean absolute error (MAE) relative to experiment of more than 0.5 eV. Generally speaking, the double IP values increase with the size of the basis set, and DCB-X2C-DIP-EOMCCSD seems to agree best with experiment when combined with the triple-zeta-quality basis set (the MAE is 0.135 eV in this case). On the other hand, increasing the basis set to the quadruple-zeta level, followed by the full ANO-RCC basis set leads to larger MAE values (0.175 eV and 0.269 eV, respectively). The fact that large-basis DCB-X2C-DIP-EOMCCSD overestimates the double IPs reflects the fact that DCB-X2C-DIP-EOMCCSD is not converged with respect to the correlation treatment. We observe similar qualitative trends for DCB-X2C-DIP-EOMCCSD calculations carried out using other basis set families. Double IPs are underestimated using the smallest Dyall-type (dyall.acvdz) and x2c-type (x2c-SVPall-2c) basis sets (with MAEs of 0.204 eV and 0.661 eV, respectively), and the double IP values increase with increasing basis set size. At the triple-zeta level, the MAEs calculated using the dyall.acvtz and x2c-TZVPall-2c basis sets fall to 0.159 eV and 0.149 eV, respectively.

In addition to absolute double IP values, it is useful to consider the accuracy of DCB-X2C-DIP-EOMCCSD for predicting excitation energies in doubly ionized species, *i.e.*, the energy gaps between the lowest-energy state and the higher-energy states. Figure 2 provides the energy gaps correspond-

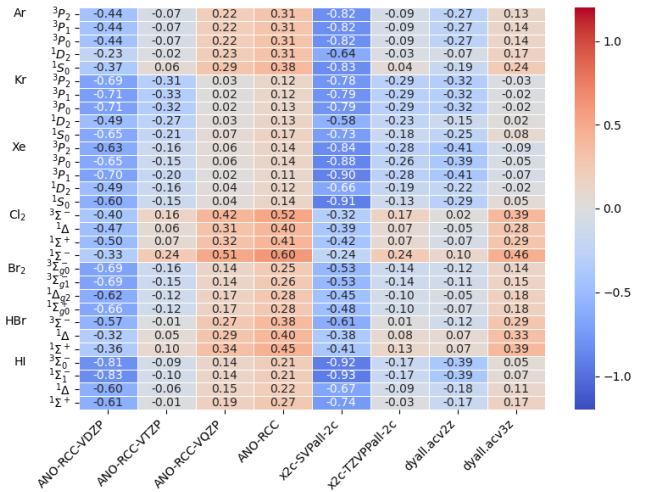


FIG. 1. Errors in double ionization potentials (eV) calculated using ANO-RCC-VnZP ( $n = D, T, Q$ ), X2C- $n$ ZVPPall-2c ( $n = D, T$ ), and Dyall-acvnn ( $n = D, T$ ) basis sets.

ing to the states considered in Fig. 1, using the same basis sets and correlation spaces. Unlike the absolute double IPs, we observe a clear trend indicating that the quality of the energy gaps improves with increasing basis set size. For example, proceeding through the ANO-RCC family, the MAEs in the energy gaps compared to experiment are 0.089 eV (ANO-RCC-DZVP), 0.046 eV (ANO-RCC-TZVP), 0.032 eV (ANO-RCC-QZVP), and 0.031 eV (full ANO-RCC). We see similar improvements in the MAEs when moving from double-zeta to triple-zeta quality sets using the x2c-type (0.090 eV to 0.062 eV) and Dyall-type (0.089 eV to 0.057 eV) basis sets. As stated above, the remaining error in the large-basis energy gaps is due to correlation effects that are missing at the DCB-X2C-DIP-EOMCCSD level of theory.

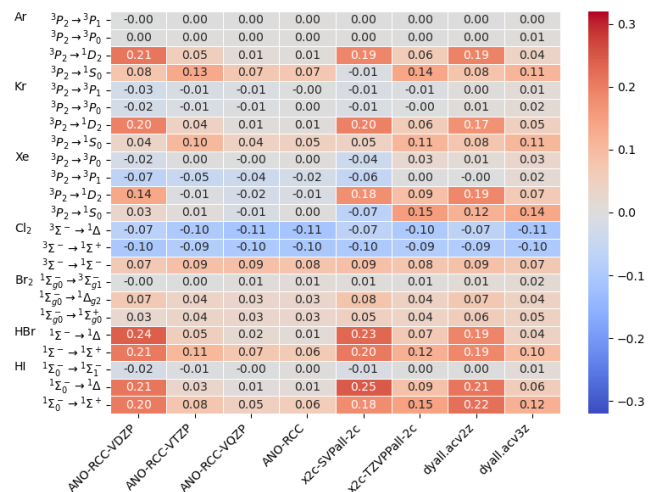


FIG. 2. Errors in excitation energies (eV) for doubly ionized systems calculated using ANO-RCC-VnZP ( $n = D, T, Q$ ), X2C- $n$ ZVPPall-2c ( $n = D, T$ ), and Dyall-acvanz ( $n = D, T$ ) basis sets.

The data discussed thus far indicate that DCB-X2C-DIP-EOMCCSD calculations carried out in large basis sets do not provide accurate predictions of experimentally-obtained double IP values for the systems considered in this work. In the full ANO-RCC basis set DCB-X2C-DIP-EOMCCSD overestimates the double IP values by 0.1–0.6 eV. Given the good agreement between mmfX2C- and 4c-DIP-EOMCCSD calculations in Table I, we conclude that the poor performance of DCB-X2C-DIP-EOMCCSD stems not from the relativistic treatment but, rather, from a lack of higher-order correlation effects that are missing at this level of theory. To remedy the situation, we adopt the following composite protocol to approximately account for higher-order correlation effects missing at the DCB-X2C-DIP-EOMCCSD level of theory. We define

$$DIP_K = DIP_K^{\text{SD/full}} + \left[ DIP_K^{\text{SDT/DZ}} - DIP_K^{\text{SD/DZ}} \right] \quad (9)$$

The first term on the right-hand side of Eq. 9 represents the double IP value obtained using DCB-X2C-DIP-EOMCCSD within the full ANO-RCC basis, and the subsequent terms correspond to the difference between DCB-X2C-DIP-EOMCCSDT and DCB-X2C-DIP-EOMCCSD double IP values evaluated within ANO-RCC-VDZP basis set.

Errors in double IP values for atomic systems that were computed using DCB-X2C-DIP-EOMCCSD / ANO-RCC and via Eq. 9 are tabulated in Table III. In general, higher-order correlation effects captured by DCB-X2C-DIP-EOMCCSDT substantially reduce the errors in the double IP values from DCB-X2C-DIP-EOMCCSD, sometimes by more than an order of magnitude. For example, for the argon atom, DCB-X2C-DIP-EOMCCSD overestimates the double IP values by more than 0.3 eV, while, for some states ( $^3P_2$ ,  $^3P_1$ ,  $^3P_0$ , and  $^1D_2$ ), higher-order correlation effects reduce these errors to only -0.001 eV – 0.005 eV. For the remaining state of the argon atom ( $^1S_0$ ) the improvement is smaller but still impressive, reducing the error by more than a factor of four (0.379 eV to 0.090 eV). For krypton and xenon atoms, DCB-X2C-DIP-EOMCCSD overestimates the double IP values by more than 0.1 eV. Higher-order correlation effects reduce the magnitudes of these errors to well below 0.05 eV for krypton (2.6 – 4.8 fold improvement) and to below 0.02 eV for xenon (6.1 – 15.4 fold improvement). Note that, while large-basis DCB-X2C-DIP-EOMCCSD double IPs are always upper bounds to the experimentally obtained values, the error in double IPs from the composite method displays no clear trend in terms of sign.

## V. CONCLUSIONS

We have implemented relativistic formulations of DIP-EOMCCSD and DIP-EOMCCSDT within the 1eX2C and DC-, DCG-, and DCB-X2C frameworks. Direct comparisons against full 4c-DIP-EOMCCSD calculations show excellent agreement with DC(G)-X2C-DIP-EOMCCSD, suggesting, at least for the systems studied herein, two-electron relativistic effects are well-described by the mean-field treatment in mmfX2C, and remaining relativistic two-electron and

TABLE III. Experimentally-obtained double IP values (eV)<sup>97</sup> and errors in double IP values (eV) calculated using DCB-X2C-DIP-EOMCCSD in the ANO-RCC basis set (labeled SD) and via Eq. 9 (labeled SDT).

	State	SD	SDT	experiment
Ar	$^3P_2$	0.307	0.000	43.389
	$^3P_1$	0.309	-0.001	43.527
	$^3P_0$	0.311	0.000	43.584
	$^1D_2$	0.313	0.005	45.126
	$^1S_0$	0.379	0.090	47.514
Kr	$^3P_2$	0.125	-0.036	38.359
	$^3P_1$	0.124	-0.047	38.923
	$^3P_0$	0.127	-0.043	39.018
	$^1D_2$	0.133	-0.028	40.175
	$^1S_0$	0.173	0.043	42.461
Xe	$^3P_2$	0.135	0.016	33.105
	$^3P_1$	0.139	0.009	34.113
	$^3P_0$	0.110	-0.018	34.319
	$^1D_2$	0.123	-0.015	35.225
	$^1S_0$	0.138	-0.016	37.581

electron-positron correlation effects are negligible. A subsequent basis set study on vertical double IPs for noble gas and diatomic species has shown that DCB-DIP-EOMCCSD tends to overestimate double IP values in the limit of a complete one-electron basis, by more than 0.25 eV, on average. For atomic systems, we were able to demonstrate that a composite scheme whereby the dominant correlation effects are captured by large-basis DCB-DIP-EOMCCSD and remaining high-order correlation effects are approximately modeled via small-basis DCB-DIP-EOMCCSDT brings the double IP values into excellent agreement with experiment; for Xe atom, for example, absolute errors in double IP values from this approach are less than 0.02 eV.

**Supporting Information** Double ionization potentials from all-electron versus frozen core DCB-X2C-DIP-EOMCCSD calculations, as well as double ionization potentials and excitation energies of doubly ionized species computed using 1eX2C- and DCB-X2C-DIP-EOMCCSD within the frozen core approximation.

## ACKNOWLEDGMENTS

This material is based upon work supported by the U.S. Department of Energy, Office of Science, Office of Advanced Scientific Computing Research and Office of Basic Energy Sciences, Scientific Discovery through the Advanced Computing (SciDAC) program under Award No. DE-SC0022263. The Chronus Quantum software infrastructure development is supported by the Office of Advanced Cyberinfrastructure, National Science Foundation (Grant Nos. OAC-2103717 and OAC-2103705). This project used resources of the National Energy Research Scientific Computing Center, a DOE Office

of Science User Facility supported by the Office of Science of the U.S. DOE under Contract No. DE-AC02-05CH11231 using NERSC award ERCAP-0027762 and ERCAP-0032454.

- <sup>1</sup>F. Coester, "Bound states of a many-particle system," *Nucl. Phys.* **7**, 421–424 (1958).
- <sup>2</sup>F. Coester and H. Kümmel, "Short-range correlations in nuclear wave functions," *Nucl. Phys.* **17**, 477–485 (1960).
- <sup>3</sup>J. Čížek, "On the correlation problem in atomic and molecular systems. calculation of wavefunction components in ursell-type expansion using quantum-field theoretical methods," *J. Chem. Phys.* **45**, 4256–4266 (1966).
- <sup>4</sup>J. Čížek, "On the use of the cluster expansion and the technique of diagrams in calculations of correlation effects in atoms and molecules," *Adv. Chem. Phys.* **14**, 35–89 (1969).
- <sup>5</sup>J. Paldus, J. Čížek, and I. Shavitt, "Correlation problems in atomic and molecular systems. iv. extended coupled-pair many-electron theory and its application to the  $\text{bh}_3$  molecule," *Phys. Rev. A* **5**, 50–67 (1972).
- <sup>6</sup>J. Paldus and X. Li, "A critical assessment of coupled cluster method in quantum chemistry," *Adv. Chem. Phys.* **110**, 1–175 (1999).
- <sup>7</sup>R. J. Bartlett and M. Musiał, "Coupled-cluster theory in quantum chemistry," *Rev. Mod. Phys.* **79**, 291–352 (2007).
- <sup>8</sup>G. D. Purvis and R. J. Bartlett, "A full coupled-cluster singles and doubles model: The inclusion of disconnected triples," *J. Chem. Phys.* **76**, 1910–1918 (1982).
- <sup>9</sup>J. M. Cullen and M. C. Zerner, "The linked singles and doubles model: An approximate theory of electron correlation based on the coupled-cluster ansatz," *J. Chem. Phys.* **77**, 4088–4109 (1982).
- <sup>10</sup>J. Noga and R. J. Bartlett, "The full CCSDT model for molecular electronic structure," *J. Chem. Phys.* **86**, 7041–7050 (1987), **89**, 3401 (1988) [Erratum].
- <sup>11</sup>G. E. Scuseria and H. F. Schaefer, "A new implementation of the full ccisd model for molecular electronic structure," *Chem. Phys. Lett.* **152**, 382–386 (1988).
- <sup>12</sup>K. Emrich, "An extension of the coupled cluster formalism to excited states (I)," *Nucl. Phys. A* **351**, 379–396 (1981).
- <sup>13</sup>J. Geertsen, M. Ritby, and R. J. Bartlett, "The equation-of-motion coupled-cluster method: Excitation energies of  $\text{be}$  and  $\text{co}$ ," *Chem. Phys. Lett.* **164**, 57–62 (1989).
- <sup>14</sup>J. F. Stanton and R. J. Bartlett, "The equation of motion coupled-cluster method. a systematic biorthogonal approach to molecular excitation energies, transition probabilities, and excited state properties," *J. Chem. Phys.* **98**, 7029–7039 (1993).
- <sup>15</sup>H. J. Monkhorst, "Calculation of properties with the coupled-cluster method," *Int. J. Quantum Chem.* **12**, 421–432 (1977).
- <sup>16</sup>E. Dalggaard and H. J. Monkhorst, "Some aspects of the time-dependent coupled-cluster approach to dynamic response functions," *Phys. Rev. A* **28**, 1217–1222 (1983).
- <sup>17</sup>D. Mukherjee and P. Mukherjee, "A response-function approach to the direct calculation of the transition-energy in a multiple-cluster expansion formalism," *Chem. Phys.* **39**, 325–335 (1979).
- <sup>18</sup>H. Sekino and R. J. Bartlett, "A linear response, coupled-cluster theory for excitation energy," *Int. J. Quantum Chem.* **26**, 255–265 (1984).
- <sup>19</sup>M. Takahashi and J. Paldus, "Time-dependent coupled cluster approach: Excitation energy calculation using an orthogonally spin-adapted formalism," *J. Chem. Phys.* **85**, 1486–1501 (1986).
- <sup>20</sup>H. Koch and P. Jørgensen, "Coupled cluster response functions," *J. Chem. Phys.* **93**, 3333–3344 (1990).
- <sup>21</sup>H. Koch, H. J. A. Jensen, P. Jørgensen, and T. Helgaker, "Excitation energies from the coupled cluster singles and doubles linear response function (ccsdlr). applications to  $\text{be}$ ,  $\text{ch}^+$ ,  $\text{co}$ , and  $\text{h}_2\text{o}$ ," *J. Chem. Phys.* **93**, 3345–3350 (1990).
- <sup>22</sup>H. Nakatsuji, "Cluster expansion of the wavefunction. Calculation of electron correlations in ground and excited states by SAC and SAC CI theories," *Chem. Phys. Lett.* **67**, 334–342 (1979).
- <sup>23</sup>P. Piecuch and K. Kowalski, "The State-Universal Multi-Reference Coupled-Cluster Theory: An Overview of Some Recent Advances," *Int. J. Mol. Sci.* **3**, 676–709 (2002).
- <sup>24</sup>D. I. Lyakh, M. Musiał, V. F. Lotrich, and R. J. Bartlett, "Multireference Nature of Chemistry: The Coupled-Cluster View," *Chem. Rev.* **112**, 182–243 (2012).
- <sup>25</sup>F. A. Evangelista, "Perspective: Multireference coupled cluster theories of dynamical electron correlation," *J. Chem. Phys.* **149**, 030901 (2018).
- <sup>26</sup>D. Casanova, L. V. Slipchenko, A. I. Krylov, and M. Head-Gordon, "Double spin-flip approach within equation-of-motion coupled cluster and configuration interaction formalisms: Theory, implementation, and examples," *J. Chem. Phys.* **130**, 044103 (2009).
- <sup>27</sup>A. I. Krylov, "Size-consistent wave functions for bond-breaking: The equation-of-motion spin-flip model," *Chem. Phys. Lett.* **338**, 375–384 (2001).
- <sup>28</sup>A. I. Krylov, "Spin-Flip Equation-of-Motion Coupled-Cluster Electronic Structure Method for a Description of Excited States, Bond Breaking, Di-radicals, and Tri-radicals," *Acc. Chem. Res.* **39**, 83–91 (2006).
- <sup>29</sup>A. I. Krylov, "Equation-of-motion coupled-cluster methods for open-shell and electronically excited species: The hitchhiker's guide to fock space," *Annu. Rev. Phys. Chem.* **59**, 433–462 (2008).
- <sup>30</sup>R. J. Bartlett and J. F. Stanton, "Applications of Post-Hartree-Fock Methods: A Tutorial," *5*, 65–169 (1994).
- <sup>31</sup>M. Nooijen and J. G. Snijders, "Coupled cluster approach to the single-particle green's function," *Int. J. Quantum Chem.* **44**, 55–83 (1992).
- <sup>32</sup>M. Nooijen and J. G. Snijders, "Coupled cluster green's function method: Working equations and applications," *Int. J. Quantum Chem.* **48**, 15–48 (1993).
- <sup>33</sup>J. F. Stanton and J. Gauss, "Analytic energy derivatives for ionized states described by the equation-of-motion coupled cluster method," *J. Chem. Phys.* **101**, 8938–8944 (1994).
- <sup>34</sup>M. Musiał, S. A. Kucharski, and R. J. Bartlett, "Equation-of-motion coupled cluster method with full inclusion of the connected triple excitations for ionized states: IP-EOM-CCSDT," *J. Chem. Phys.* **118**, 1128–1136 (2003).
- <sup>35</sup>M. Musiał and R. J. Bartlett, "EOM-CCSDT study of the low-lying ionization potentials of ethylene, acetylene and formaldehyde," *Chem. Phys. Lett.* **384**, 210–214 (2004).
- <sup>36</sup>Y. J. Bomble, J. C. Saeh, J. F. Stanton, P. G. Szalay, M. Kállay, and J. Gauss, "Equation-of-motion coupled-cluster methods for ionized states with an approximate treatment of triple excitations," *J. Chem. Phys.* **122**, 154107 (2005).
- <sup>37</sup>J. R. Gour, P. Piecuch, and M. Włoch, "Active-space equation-of-motion coupled-cluster methods for excited states of radicals and other open-shell systems: EA-EOMCCSDt and IP-EOMCCSDt," *J. Chem. Phys.* **123**, 134113 (2005).
- <sup>38</sup>J. R. Gour, P. Piecuch, and M. Włoch, "Extension of the active-space equation-of-motion coupled-cluster methods to radical systems: The EA-EOMCCSDt and IP-EOMCCSDt approaches," *Int. J. Quantum Chem.* **106**, 2854–2874 (2006).
- <sup>39</sup>J. R. Gour and P. Piecuch, "Efficient formulation and computer implementation of the active-space electron-attached and ionized equation-of-motion coupled-cluster methods," *J. Chem. Phys.* **125**, 234107 (2006).
- <sup>40</sup>M. Nooijen and R. J. Bartlett, "Equation of motion coupled cluster method for electron attachment," *J. Chem. Phys.* **102**, 3629–3647 (1995).
- <sup>41</sup>M. Nooijen and R. J. Bartlett, "Description of core-excitation spectra by the open-shell electron-attachment equation-of-motion coupled cluster method," *J. Chem. Phys.* **102**, 6735–6756 (1995).
- <sup>42</sup>M. Musiał and R. J. Bartlett, "Equation-of-motion coupled cluster method with full inclusion of connected triple excitations for electron-attached states: EA-EOM-CCSDT," *J. Chem. Phys.* **119**, 1901–1908 (2003).
- <sup>43</sup>M. Władysławski and M. Nooijen, "The Photoelectron Spectrum of the  $\text{NO}_3$  Radical Revisited: A Theoretical Investigation of Potential Energy Surfaces and Conical Intersections," in *Low-Lying Potential Energy Surfaces*, ACS Symposium Series, Vol. 828 (2002) Chap. 4, pp. 65–92.
- <sup>44</sup>M. Nooijen, "State Selective Equation of Motion Coupled Cluster Theory: Some Preliminary Results," *Int. J. Mol. Sci.* **3**, 656–675 (2002).
- <sup>45</sup>M. Musiał, A. Perera, and R. J. Bartlett, "Multireference coupled-cluster theory: The easy way," *J. Chem. Phys.* **134**, 114108 (2011).
- <sup>46</sup>T. Kuś and A. I. Krylov, "Using the charge-stabilization technique in the double ionization potential equation-of-motion calculations with dianion references," *J. Chem. Phys.* **135**, 084109 (2011).

<sup>47</sup>T. Kuš and A. I. Krylov, “De-perturbative corrections for charge-stabilized double ionization potential equation-of-motion coupled-cluster method,” *J. Chem. Phys.* **136**, 244109 (2012).

<sup>48</sup>J. Shen and P. Piecuch, “Doubly electron-attached and doubly ionized equation-of-motion coupled-cluster methods with 4-particle–2-hole and 4-hole–2-particle excitations and their active-space extensions,” *J. Chem. Phys.* **138**, 194102 (2013).

<sup>49</sup>J. Shen and P. Piecuch, “Doubly electron-attached and doubly ionised equation-of-motion coupled-cluster methods with full and active-space treatments of 4-particle–2-hole and 4-hole–2-particle excitations: The role of orbital choices,” *Mol. Phys.* **112**, 868–885 (2014).

<sup>50</sup>K. Gururangan, A. K. Dutta, and P. Piecuch, “Double ionization potential equation-of-motion coupled-cluster approach with full inclusion of 4-hole–2-particle excitations and three-body clusters,” *J. Chem. Phys.* **162**, 061101 (2025).

<sup>51</sup>K. G. Dyall, “Interfacing relativistic and nonrelativistic methods. I. Normalized elimination of the small component in the modified Dirac equation,” *J. Chem. Phys.* **106**, 9618–9626 (1997).

<sup>52</sup>K. G. Dyall, “Interfacing relativistic and nonrelativistic methods. II. investigation of a low-order approximation,” *J. Chem. Phys.* **109**, 4201–4208 (1998).

<sup>53</sup>K. G. Dyall and T. Enevoldsen, “Interfacing relativistic and nonrelativistic methods. III. atomic 4-spinor expansions and integral approximations,” *J. Chem. Phys.* **111**, 10000–10007 (1999).

<sup>54</sup>K. G. Dyall, “Interfacing relativistic and nonrelativistic methods. IV. One- and two-electron scalar approximations,” *J. Chem. Phys.* **115**, 9136–9143 (2001).

<sup>55</sup>M. Filatov and D. Cremer, “A new quasi-relativistic approach for density functional theory based on the normalized elimination of the small component,” *Chem. Phys. Lett.* **351**, 259–266 (2002).

<sup>56</sup>W. Kutzelnigg and W. Liu, “Quasirelativistic theory equivalent to fully relativistic theory,” *J. Chem. Phys.* **123**, 241102 (2005).

<sup>57</sup>W. Liu and D. Peng, “Infinite-order quasirelativistic density functional method based on the exact matrix quasirelativistic theory,” *J. Chem. Phys.* **125**, 044102 (2006).

<sup>58</sup>D. Peng, W. Liu, Y. Xiao, and L. Cheng, “Making four- and two-component relativistic density functional methods fully equivalent based on the idea of from atoms to molecule,” *J. Chem. Phys.* **127**, 104106 (2007).

<sup>59</sup>M. Iliǎš and T. Saue, “An infinite-order relativistic hamiltonian by a simple one-step transformation,” *J. Chem. Phys.* **126**, 064102 (2007).

<sup>60</sup>W. Liu and D. Peng, “Exact two-component hamiltonians revisited,” *J. Chem. Phys.* **131**, 031104 (2009).

<sup>61</sup>W. Liu, “Ideas of relativistic quantum chemistry,” *Mol. Phys.* **108**, 1679–1706 (2010).

<sup>62</sup>Z. Li, Y. Xiao, and W. Liu, “On the spin separation of algebraic two-component relativistic hamiltonians,” *J. Chem. Phys.* **137**, 154114 (2012).

<sup>63</sup>D. Peng, N. Middendorf, F. Weigend, and M. Reiher, “An efficient implementation of two-component relativistic exact-decoupling methods for large molecules,” *J. Chem. Phys.* **138**, 184105 (2013).

<sup>64</sup>F. Egidi, J. J. Goings, M. J. Frisch, and X. Li, “Direct Atomic-Orbital-Based Relativistic Two-Component Linear Response Method for Calculating Excited-State Fine Structures,” *J. Chem. Theory Comput.* **12**, 3711–3718 (2016).

<sup>65</sup>J. J. Goings, J. M. Kasper, F. Egidi, S. Sun, and X. Li, “Real time propagation of the exact two component time-dependent density functional theory,” *J. Chem. Phys.* **145**, 104107 (2016).

<sup>66</sup>L. Konecny, M. Kadek, S. Komorovsky, O. L. Malkina, K. Ruud, and M. Repisky, “Acceleration of Relativistic Electron Dynamics by Means of X2C Transformation: Application to the Calculation of Nonlinear Optical Properties,” *J. Chem. Theory Comput.* **12**, 5823–5833 (2016).

<sup>67</sup>F. Egidi, S. Sun, J. J. Goings, G. Scalmani, M. J. Frisch, and X. Li, “Two-Component Noncollinear Time-Dependent Spin Density Functional Theory for Excited State Calculations,” *J. Chem. Theory Comput.* **13**, 2591–2603 (2017).

<sup>68</sup>J. Liu and L. Cheng, “Relativistic coupled-cluster and equation-of-motion coupled-cluster methods,” *WIREs Comput. Mol. Sci.* **11**, e1536 (2021).

<sup>69</sup>P. Sharma, A. J. Jenkins, G. Scalmani, M. J. Frisch, D. G. Truhlar, L. Gagliardi, and X. Li, “Exact-Two-Component Multiconfiguration Pair-Density Functional Theory,” *J. Chem. Theory Comput.* **18**, 2947–2954 (2022).

<sup>70</sup>L. Lu, H. Hu, A. J. Jenkins, and X. Li, “Exact-Two-Component Relativistic Multireference Second-Order Perturbation Theory,” *J. Chem. Theory Comput.* **18**, 2983–2992 (2022).

<sup>71</sup>C. E. Hoyer, H. Hu, L. Lu, S. Knecht, and X. Li, “Relativistic Kramers-Unrestricted Exact-Two-Component Density Matrix Renormalization Group,” *J. Phys. Chem. A* **126**, 5011–5020 (2022).

<sup>72</sup>T. Zhang, S. Banerjee, L. N. Koulias, E. F. Valeev, A. E. DePrince III, and X. Li, “Dirac–Coulomb–Breit Molecular Mean-Field Exact-Two-Component Relativistic Equation-of-Motion Coupled-Cluster Theory,” *J. Phys. Chem. A* **128**, 3408–3418 (2024).

<sup>73</sup>M. Kovtun, E. Lambros, A. Liu, D. Tang, D. B. Williams-Young, and X. Li, “Accelerating relativistic exact-two-component density functional theory calculations with graphical processing units,” *J. Chem. Theory Comput.* **20**, 7694–7699 (2024).

<sup>74</sup>H. Hu, S. Upadhyay, L. Lu, A. J. Jenkins, T. Zhang, A. Shayit, S. Knecht, and X. Li, “Small Tensor Product Distributed Active Space (STP-DAS) Framework for Relativistic and Non-relativistic Multiconfiguration Calculations: Scaling from  $10^9$  on a Laptop to  $10^{12}$  Determinants on a Supercomputer,” *Comput. Phys. Rep.* **5**, 041404 (2024).

<sup>75</sup>Z. Wang, S. Hu, F. Wang, and J. Guo, “Equation-of-motion coupled-cluster method for doubly ionized states with spin-orbit coupling,” *J. Chem. Phys.* **142**, 144109 (2015).

<sup>76</sup>H. Zhao, Z. Wang, M. Guo, and F. Wang, “Splittings of d8 configurations of late-transition metals with EOM-DIP-CCSD and FSCCSD methods,” *J. Chem. Phys.* **152**, 134105 (2020).

<sup>77</sup>H. Pathak, S. Sasmal, M. K. Nayak, N. Vaval, and S. Pal, “Relativistic equation-of-motion coupled-cluster method for the ionization problem: Application to molecules,” *Phys. Rev. A* **90**, 062501 (2014).

<sup>78</sup>H. Pathak, S. Sasmal, K. Talukdar, M. K. Nayak, N. Vaval, and S. Pal, “Relativistic double-ionization equation-of-motion coupled-cluster method: Application to low-lying doubly ionized states,” *J. Chem. Phys.* **152**, 104302 (2020).

<sup>79</sup>J. C. Boettger, “Approximate two-electron spin-orbit coupling term for density-functional-theory DFT calculations using the Douglas–Kroll–Hess transformation,” *Phys. Rev. B* **62**, 7809–7815 (2000).

<sup>80</sup>J. Ehrman, E. Martinez-Baez, A. J. Jenkins, and X. Li, “Improving One-Electron Exact-Two-Component Relativistic Methods with the Dirac–Coulomb–Breit–Parameterized Effective Spin–Orbit Coupling,” *J. Chem. Theory Comput.* **19**, 5785–5790 (2023).

<sup>81</sup>J. Sikkema, L. Visscher, T. Saue, and M. Iliǎš, “The molecular mean-field approach for correlated relativistic calculations,” *J. Chem. Phys.* **131**, 124116 (2009).

<sup>82</sup>S. H. Yuwono, R. R. Li, T. Zhang, X. Li, and I. DePrince, A. Eugene, “Two-component relativistic equation-of-motion coupled cluster for electron ionization,” *J. Chem. Phys.* **162**, 084110 (2025).

<sup>83</sup>P. Pollak and F. Weigend, “Segmented Contracted Error-Consistent Basis Sets of Double- and Triple- $\zeta$  Valence Quality for One- and Two-Component Relativistic All-Electron Calculations,” *J. Chem. Theory Comput.* **13**, 3696–3705 (2017).

<sup>84</sup>K. G. Dyall, “Relativistic and nonrelativistic finite nucleus optimized triple-zeta basis sets for the 4p, 5p and 6p elements,” *Theor. Chem. Acc.* **108**, 335–340 (2002), **109**, 284 (2003) [Erratum].

<sup>85</sup>K. G. Dyall, “Relativistic Quadruple-Zeta and Revised Triple-Zeta and Double-Zeta Basis Sets for the 4p, 5p, and 6p Elements,” *Theor. Chem. Acc.* **115**, 441–447 (2006).

<sup>86</sup>K. G. Dyall, “Relativistic double-zeta, triple-zeta, and quadruple-zeta basis sets for the light elements H–Ar,” *Theor. Chem. Acc.* **135**, 128 (2016).

<sup>87</sup>K. G. Dyall, “Core correlating basis functions for elements 31–118,” *Theor. Chem. Acc.* **131**, 1217 (2012).

<sup>88</sup>K. G. Dyall, “Relativistic double-zeta, triple-zeta, and quadruple-zeta basis sets for the 7p elements, with atomic and molecular applications,” *Theor. Chem. Acc.* **131**, 1–20 (2012).

<sup>89</sup>K. G. Dyall, “Dyall dz, tz, and qz basis sets for relativistic electronic structure calculations,” Last accessed November 11, 2024.

<sup>90</sup>B. O. Roos, R. Lindh, P.-Å. Malmqvist, V. Veryazov, and P.-O. Widmark, “New Relativistic ANO Basis Sets for Transition Metal Atoms,” *J. Phys. Chem. A* **109**, 6575–6579 (2005).

<sup>91</sup>B. O. Roos, R. Lindh, P.-Å. Malmqvist, V. Veryazov, and P.-O. Widmark, “Main group atoms and dimers studied with a new relativistic ano basis

set,” *J. Phys. Chem. A* **108**, 2851–2858 (2004).

<sup>92</sup>A. E. DePrince III and C. D. Sherrill, “Accuracy and efficiency of coupled-cluster theory using density fitting/cholesky decomposition, frozen natural orbitals, and a t1-transformed hamiltonian,” *J. Chem. Theory Comput.* **9**, 2687–2696 (2013).

<sup>93</sup>D. B. Williams-Young, A. Petrone, S. Sun, T. F. Stetina, P. Lestrange, C. E. Hoyer, D. R. Nascimento, L. Koulias, A. Wildman, J. Kasper, J. J. Goings, F. Ding, A. E. DePrince III, E. F. Valeev, and X. Li, “The chronus quantum software package,” *WIREs Comput. Mol. Sci.* **10**, e1436 (2020).

<sup>94</sup>J. A. Calvin and E. F. Valeev, “Tiledarray: A general-purpose scalable block-sparse tensor framework,” Last accessed June 10, 2024.

<sup>95</sup>N. C. Rubin and A. E. DePrince III, “p<sup>†</sup>q: a tool for prototyping many-body methods for quantum chemistry,” *Mol. Phys.* **119**, e1954709 (2021).

<sup>96</sup>M. D. Liebenthal, S. H. Yuwono, L. N. Koulias, R. R. Li, N. C. Rubin, and A. E. DePrince III, “Automated quantum chemistry code generation with the p<sup>†</sup>q package,” arXiv preprint , 2501.08882 (2025).

<sup>97</sup>A. Kramida, Yu. Ralchenko, J. Reader, and and NIST ASD Team, NIST Atomic Spectra Database (ver. 5.12), [Online]. Available: <https://physics.nist.gov/asd> [2025, March 18]. National Institute of Standards and Technology, Gaithersburg, MD. (2024).

<sup>98</sup>A. G. McConkey, G. Dawber, L. Avaldi, M. A. MacDonald, G. C. King, and R. I. Hall, “Threshold photoelectrons coincidence spectroscopy of doubly charged ions of hydrogen chloride and chlorine,” *J. Phys. B: At. Mol. Opt. Phys.* **27**, 271 (1994).

<sup>99</sup>T. Fleig, D. Edvardsson, S. T. Banks, and J. H. Eland, “A theoretical and experimental study of the double photoionisation of molecular bromine and a new double ionisation mechanism,” *Chem. Phys.* **343**, 270–280 (2008).

<sup>100</sup>J. H. Eland, “Complete double photoionisation spectra of small molecules from tof-pepeco measurements,” *Chem. Phys.* **294**, 171–186 (2003).

<sup>101</sup>A. J. Yencha, A. M. Juarez, S. Pui Lee, G. C. King, F. R. Bennett, F. Kemp, and I. R. McNab, “Photo-double ionization of hydrogen iodide: experiment and theory,” *Chem. Phys.* **303**, 179–187 (2004).